Article ID: 1006-8775(2011) 03-0221-10

# MODIS BRIGHTNESS TEMPERATURE DATA ASSIMILATION UNDER CLOUDY CONDITIONS Ⅱ: IMPACTS ON RAINSTORM FORECASTING

DING Wei-yu (丁伟钰), WAN Qi-lin (万齐林), HUANG Yan-yan (黄燕燕), CHEN Zi-tong (陈子通), ZHANG Cheng-zhong (张诚忠)

(Guangzhou Institute of Tropical and Marine Meteorology, CMA, Guangzhou 510080 China)

**Abstract:** Satellite observations provide large amount of information of clouds and precipitation and play an important role in the forecast of heavy rainfall. However, we have not fully taken advantage of satellite observations in the data assimilation of numerical weather predictions, especially those in infrared channels. It is common to only assimilate radiances under clear-sky conditions since it is extremely difficult to simulate infrared transmittance in cloudy sky. On the basis of the Global and Regional Assimilation and Prediction Enhanced System 3-dimensional variance (GRAPES-3DVar), cloud liquid water content, ice-water content and cloud cover are employed as governing variables in the assimilation system. This scheme can improve the simulation of infrared transmittance by a fast radiative transfer model for TOVS (RTTOV) and adjust the atmospheric and cloud parameters based on infrared radiance observations. In this paper, we investigate a heavy rainfall over Guangdong province on May 26, 2007, which is right after the onset of a South China Sea monsoon. In this case, channels of the Moderate Resolution Imaging Spectroradiometer (MODIS) for observing water vapor (Channel 27) and cloud top altitude (Channel 36) are selected for the assimilation. The process of heavy rainfall is simulated by the Weather Research and Forecasting (WRF) model. Our results show that the assimilated MODIS data can improve the distribution of water vapor and temperature in the first guess field and indirectly adjust the upper-level wind field. The tendency of adjustment agrees well with the satellite observations. The assimilation scheme has positive impacts on the short-range forecasting of rainstorm.

**Key words:** MODIS brightness temperature data; assimilation; rainstorm

**CLC number:** P412.27 **Document code:** A **doi:** 10.3969/j.issn.1006-8775.2011.03.004

## 1 INTRODUCTION

Satellite data are playing an important role in monitoring and forecasting heavy rainfall. Being high in both time and space resolution, they offer opportunity for continuous observation of the formation of cloud systems and exploration of the relationships between the evolution of weather systems and precipitation[1, 2]. Heavy rainfall and severe convective weather are so small in the spatio-temporal scale that they can hardly be captured by conventional means. With the use of satellite data, meso- and fine-scale clouds can be covered for their entire lifecycle from formation and development through getting matured and dissipated. In addition, distribution of large-scale cloud systems can also be observed[3]. It is well known that weather systems associated with heavy rain in the south of China are significantly convective, accompanied by active mesoscale convective systems. Studying an exceptionally heavy rain in the Yantze River basin in 1998, Shi et al.[4], using the time-longitude cross section of TBB, had a clear tracking of the main process of precipitation and the mesoscale cloud clusters above during the three episodes of the Meiyu raining season of that year. Using hourly satellite images and the analysis of cloud-top temperatures, they pointed out that $\beta$-mesoscale cloud clusters on the Meiyu front move from east to west due to the effect of terrain and the environmental field. Hourly infrared cloud imagery from GMS satellites were used to display cloud bands of heavy rain on the synoptic scale[5], with the disclosure that cloud clusters that formed frequently from precipitating cloud bands

**Received** 2010-02-25; **Revised** 2011-05-16; **Accepted** 2011-07-15
**Foundation item:** Natural Science Foundation of China (41075083); Natural Science Foundation of Guangdong Province (7035011)
**Biography:** DING Wei-yu, associate professor, primarily undertaking research on the techniques of tropical meteorology.
**Corresponding author:** DING Wei-yu, e-mail: wyding@grmc.gov.cn

were responsible for a sustained and exceptionally heavy rain in the middle reach of the Yangtze River in the last ten days of July, 1998. As shown in a study on the brightness temperature of satellites[6], heavy rainfall in the south of China is associated with repeated occurrence of mesoscale convective cloud clusters, which is attributed to the phenomenon that cloud clusters grow at the rear but decay in the front due to constant triggering of convection in front of mesoscale low pressures. This is different from the pattern for the Yangtze River valley where convective cloud clusters grow in the front while decaying at the rear. Xiong et al.[7] used the TBB data and other conventional observations to study an exceptionally heavy rainfall in the south of China in June 2005. They confirmed that the ceaseless generation and dissipation of mesoscale convective systems (MCSs) immediately caused the rain to maintain continuously.

Despite of the immense role played by satellite data in the research on heavy rain in the south of China, their application in numerical weather prediction (NWP) models has been met with great difficulty. The main reason is that clouds are quite frequently seen in the southern regions of the country and the raining weather is in the company of convective cloud clusters and severe rainfall. As clouds have direct impacts on infrared radiances transfer, it is difficult for radiative transfer models to simulate the infrared radiances transfer[8] or to obtain the distribution of cloud parameters in the atmosphere. A large number of previous studies focus on the assimilation of satellite data under clear sky or microwave data that are less affected by clouds. Examples of these include the followings. Three- and four-dimensional variational assimilation systems were used to assimilate clear-sky radiances data that are available without clouds and winds were forecast with better results (Andersson[9]). Assimilating the clear-sky radiances data from Television Infrared Observation Satellite Program (TIROS) Operational Vertical Sounder (TOVS) improved the forecast skill of models (Derber et al.[10]). The Advanced Microwave Sounding Unit (AMSU) microwave data were assimilated in an assimilation experiment on typhoon processes (Kidder et al.(11)). As satellite-borne microwave data are less than the infrared data that are measured by devices onboard the polar-orbiting and geostationary satellites, the needs of operational NWP models cannot be met if only the microwave data are assimilated. Besides, the infrared and microwave channels have focus of their own and what the channels observe can be used as constructive reference for forecasting.

Researchers are paying much attention to the assimilation of satellite data in all-weather conditions. Whether the observational operator of the assimilation system is able to simulate the infrared brightness temperatures of a cloudy sky becomes a key factor that determines whether infrared channels can be assimilated. Using the information of cloud physics from the NWP and RTTOV, Chevallier et al.[12] successfully simulated the brightness temperature at the 11-μm channel of a geostationary satellite under cloudy conditions. Employing three-dimensional parameters simulated with NWP models and the RTTOV radiances transfer model, Ding et al.[13] simulated the HIRS/3 infrared brightness temperature of Typhoon Chanchu. Their results showed that the RTTOV model with the simulated quantities of three-dimensional cloud parameters is able to reproduce the brightness temperature in some HIRS/3 channels. All of the research has shown that the infrared radiances have the potential prospective of being applied in cloudy and extreme weather conditions.

The assimilation of satellite data under all-weather conditions has received more and more attention over the past few years. An international conference was held in 2005 in the United States on the assimilation of satellite-observed clouds and precipitation for the NWP models. Ronald et al.[14] introduced the progresses made in satellite data, radiances transfer models, assimilation systems and numerical models with respect to all-weather assimilation of satellite data. Constructing the observational operators for assimilating radiances data under all-weather conditions using the radiative transfer model, gas extinction model and cloud model (for providing information of cloud physics needed in the radiative transfer model), Thomas et al.[15] assimilated the brightness temperature of GOES-9 and improved the simulation of stratus over land through four-dimensional variational assimilation. Ding et al.[16] was successful in assimilating the HIRS data by taking the cloud parameters as constants on the basis of the Global Regional Assimilation and Prediction System (GRAPES) 3-dimensional variation (3DVar), with the results indicating that the infrared information—unable to be assimilated by conventional means—can be incorporated into NWP models and has positive impacts on the forecast of precipitation.

With its multiple channels and wide spectra, Moderate Resolution Imaging Spectroradiometer (MODIS) provides retrieval products that have been playing an important role in data assimilation[17], whereas direct assimilation of brightness temperature is unavailable in cloudy condition. Based on GRAPES-3DVar, a previous session of this work[18] added cloud water content, cloud ice-water content and cloud cover as governing variables in the assimilation system and conducted experiments of ideal assimilation for 16 of the MODIS weather channels with the conditions of clear sky, complete cloud cover and partial cloud cover, respectively. This work has confirmed that the forward modeling of the

observational operator can be improved and cloud parameters and conventional meteorological elements can be adjusted by the observational operator, if both the cloud parameters and atmospheric parameters are taken as the governing variables during the assimilation of infrared radiances data. A heavy rain that happened after the outbreak of a monsoon in May 2007 was studied in this study. The rain was the result of the monsoon interacting with a low-pressure trough. Specifically, the background's description of water vapor and upper-level wind field in the troposphere deviates to some extent from that of satellite observation. By assimilating part of the MODIS channels, this work studies the effect of this assimilation on the forecast of heavy rain in the south of China as well as on the adjustment of the parameters for the atmosphere and clouds.

## 2 ANALYSIS OF THE WEATHER PROCESS

An event of sustained precipitation occurred on May 25–27, 2007 in Guangdong province that marked with small coverage and high intensity, with thunderstorms of more than Force eight on the Beaufort scale in some locations. At the night of May 25th, intense rainfall was observed in Fogang and Conghua with the average amount more than 100 mm. The intense rain then appeared in the districts of Huadu, Huangpu and Conghua of Guangzhou as well as in Gaozhou and Xinyi in the western part of the province. Heavy- to usually-heavy rain also appeared in parts of Qingyuan and Zhaoqing, with the amount as high as 173.4 mm in Huangpu and more than 100 mm in Huadu and Gaozhou. On May 27th, severe rainfall was mainly recorded in the Panyu and Yuexiu districts of Guangzhou and in the area stretching from Shunde, Zhongshan and Zhuhai. A number of towns were hit by rain of more than 100 mm with Lingshan exceeding 150.3 mm.

As shown in a monitoring report for 2007[19], on May 20th, a subtropical high pressure began to move to the east in the west Pacific, a lower-level warm and humid airflow was heading north from the Bay of Bengal, and the ridge of a prominent South Asia high pressure shifted northward, establishing the South China Sea summer monsoon (SCSSM). The rain process in question occurred at the onset of the SCSSM and in the company of highly unstable atmospheric stratification within the area of Guangdong province, as shown in the distribution of cloud imagery and cloud-derived winds from the IR1 channel of Fengyun-2C (FY-2C) weather satellite at 0000 UTC (Coordinated Universal Time, same below) on May 26th. With a southwesterly airflow of the SCSSM in dominant control over the province, convective systems developed in the central, eastern and northern parts. They stagnated and kept evolving over the Guangdong region. These convective systems enlarged, as shown by the 0600 UTC satellite cloud imagery (Fig. 1b), so that most of the province was under the control of cloud clusters and the upper troposphere had well-defined anticyclonic circulation. It reinforced the divergent outflow from these levels and became conducive to the heavy rain, a common pattern of circulation during the annually first raining season in the south of China accompanying the system that causes the rain. Besides, Guangdong was in an area of high humidity, as shown from the distribution of relative humidity as retrieved from the FY-2C (Fig. 1c). The reanalysis data of NCEP indicated that the province was then mainly under the control of a westerly flow as it was within the southwesterly field at the edge of the subtropical high as a 500-hPa upper-level trough was traveling east over the mid- and higher-latitudes of Asia and a southern branch of the westerly split over the Indochina Peninsula to affect the south of China. An 850-hPa shear stretching from central China to southern Guizhou province was moving south to affect the south of China, with the surface influenced by a frontal trough. The joint effect of the SCSSM and the low-pressure trough caused the process of severe rainfall. However, it is not supported by the NCEP reanalysis; it does not show the presence of the upper-level anticyclonic circulation over the Guangdong region. The location of the center of the 500-hPa specific humidity distribution is more to the northeast relative to the satellite imagery (Fig. 2a), which is possibly related to the relatively coarse grid resolution of the data concerned.

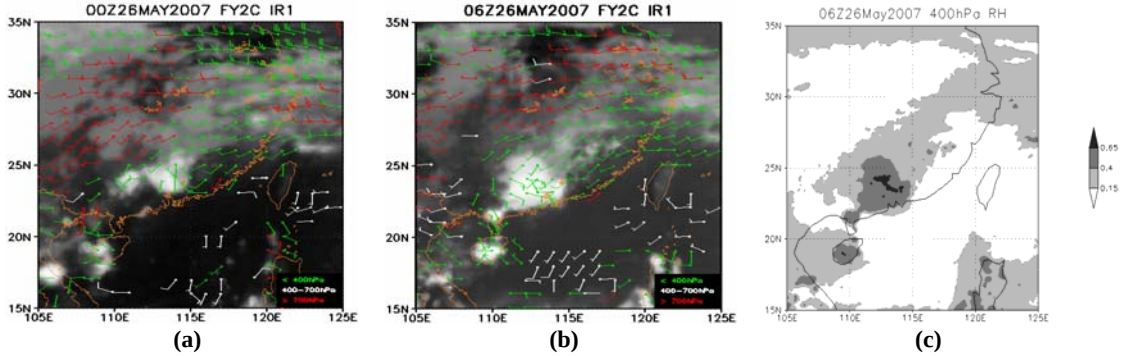


(a) (b) (c)

Fig. 1. Cloud imagery and cloud-derived winds based on the IR1 channel of FY-2C at 0000 UTC (a) and 0600 UTC (b) on May 26th and 400-hPa relative humidity retrieved by FY-2C (c).

As shown in the distribution of precipitation retrieved with quasi-real time and multiple satellite analysis from TRMM (Fig. 3), rainfall patterns are well corresponding to satellite cloud imagery. At 0000–0300 UTC on May 26th, precipitation was mainly in northern and central Guangdong. At 0600–0900 UTC, the rain spread to most of the province with the centre at the Pearl River Delta and the northwestern part of Guangdong. At 0900 UTC, the rain began to weaken and the rain band was moving northeast while weakening. This raining process lasted for just a short duration with confined area and large intensity.

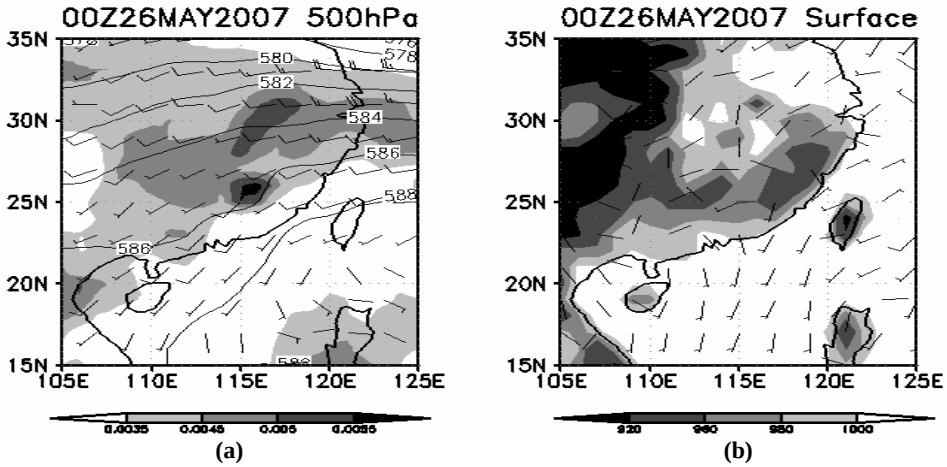


Fig. 2. 500-hPa geopotential height field (isolines), specific humidity (shaded areas) and wind fields (a) and surface pressure (shaded areas) and wind fields (b) for the NCEP reanalysis at 0000 UTC May 26, 2007.

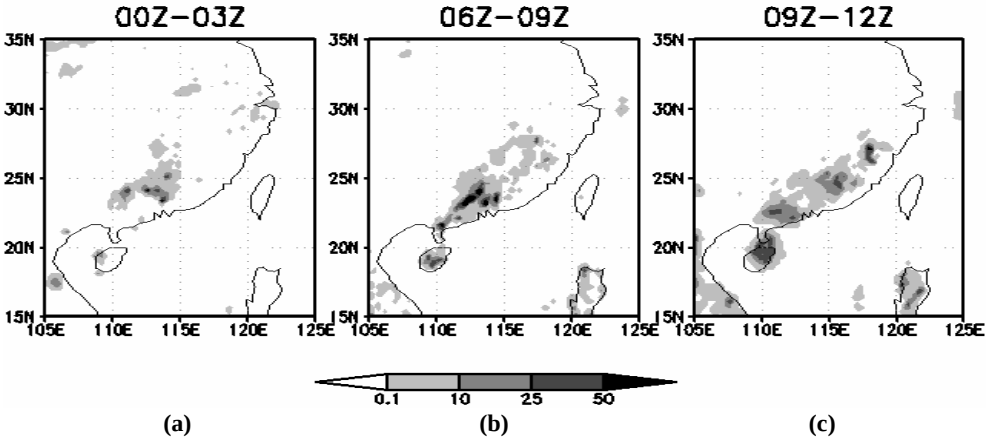


Fig. 3. Three-hour precipitation as retrieved from the TRMM quasi-real-time, multi-satellite precipiation analysis for May 26, 2007. Unit: mm. a: 0000–0300 UTC; b: 0600–0900 UTC; c: 0900–1200 UTC

## 3 DATA AND ACCOUNT OF SCHEME

The equipment onboard MODIS consists of 36 spectral bands that range from 0.4 μm (visible light) to 14.4 μm (infrared), being capable of observing the terrestrial environment, surface properties of the ocean, atmospheric clouds, radiances and aerosols, and radiation balance of the atmosphere. At 0500 UTC May 26, 2007, a heavy rain was observed over the area of Guangdong by the EOS-PM satellite (Fig. 4). According to the ideal experiment[18], assimilating the brightness temperature of Ch. 27 (6.535–6.895 μm) and Ch. 36 (14.085–14.385 μm) adjusts the background field the most under the cloudy condition. Wavelengths 6 to 7 μm are the channels of water vapor emission and those around 14 μm are the channels of cloud-top observation. As these wavelengths are highly applicable in the field of meteorology, this study assimilates the brightness temperature in these two channels to verify the assimilation effect of the scheme used here.

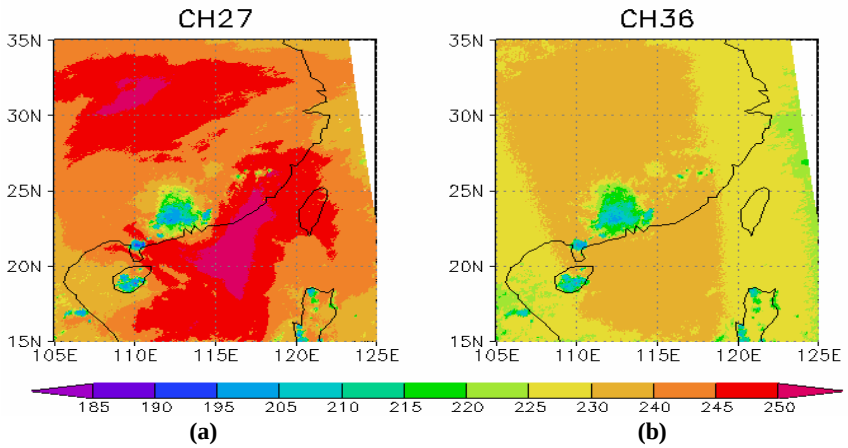


Fig. 4. Brightness temperature observed at Ch. 27 (a) and Ch. 36 (b) of MODIS for 0540 UTC May 26, 2007. Unit: K

The data used in this study is from Aqua/MODIS level 1b data at a spatial resolution of 1 km. MODIS Channels 27 and 36 are associated with the vapor emission that is received day and night. The MODIS observations are in the unit of brightness (W/(m$^2$·μm·Sr) and the Planck equation is based in this study to convert it into brightness temperature (unit: K). All MODIS radiances data in this study are brightness temperature.

The WRF model (with a resolution of 15 km) is used to simulate this process. It has 31 vertical layers and the Single-Moment 5-class scheme is used to parameterize the microphysics of clouds. This WRF scheme accounts for the water vapor, cloud water, rainwater, cloud ice and snow, with water coexisting with ice; use of the scheme makes it available a 3-dimensional field that contains cloud water content, cloud ice content and cloud cover. The NCEP reanalysis data are taken as the initial field and boundary with the data resolution at 1° ×1° . 0000 UTC May 26, 2007 is the time at which the integration begins. The forecast field six hours after the start of the integration is used as the background field of the assimilation. Physical quantities of the background field include temperature, specific humidity, $U$ and $V$ wind fields, cloud water content, cloud ice content and cloud cover, land surface types, land surface temperature, surface pressure, cloud-top pressure, total cloud cover and temperature, specific humidity and winds at the height of 2 m. For the determination of cloud-top and cloud-base position and the computation of total cloud cover, see Ding and Wan[13]. In the assimilation experiment, the MODIS data for 0540 UTC was assimilated. Then, the increment of the analysis field was superimposed to the background field. By continuing the integration through the WRF model, the rainfall process was simulated.

Due to the use of the forecast field at the sixth hour of the integration as the background field of the assimilation, some deviation exists as compared to the satellite imagery, with the most noticeable difference in the forecast field at the sixth model hour in which precipitation begins to weaken significantly in the Guangdong area and the rain band is evolving towards the northeast. As shown in the distribution of the 400-hPa background field (Fig. 5a), water vapor centers over the area connecting the Fujian and Jiangxi provinces while decreasing relatively over Guangdong. The same characteristic can be discerned from the distribution of cloud ice-water content (Fig. 5b) and cloud cover (Fig. 5c) at 400 hPa, which indicates a lower-than-0.8 cloud cover over the Guangdong area, much less than that of the area at the border between Fujian and Jiangxi. Lower-level distribution of specific humidity, cloud water content and cloud cover is also similar (Figs. 5e to 5g), with rich water vapor and dense cloud cover over the area of Fujian. As shown in the distribution of relative humidity as retrieved by the satellite FY-2C (Fig. 1c), Guangdong is still an area with high values of water vapor and receives the bulk of the rainfall at 0600 UTC, which is indicated by the distribution of relative humidity and simultaneous cloud imagery from the infrared channels of FY-2C (Fig. 1b) as well as the distribution of brightness temperature from the MODIS infrared channels (Fig. 4). Contrastive study shows that the water vapor, cloud ice-water content and cloud cover of Guangdong simulated at the sixth model hour are relatively small but they are relatively large for Fujian. Another difference between the background field and satellite observation lies in the upper tropospheric anticyclonic circulation over the Guangdong area; it is stronger at 0600 UTC than at 0000 UTC according the cloud-derived winds of the satellite but it does not exist in the background field simulated by the WRF model (Fig. 5d).

A previous ideal experiment by the authors has discovered that the addition of cloud water content, cloud ice-water content and cloud cover as governing variables in the assimilation system on

the basis of the GRAPES-3DVar runs enables the adjustment of cloud parameters and the field of conventional meteorological elements, making better use of the data. Employing the temperature, specific humidity, *U* and *V* wind fields, cloud water content, cloud ice-water content and cloud cover as the background field at the next successive time of assimilation, this study assimilates the MODIS brightness temperature through an improved assimilating system of GRAPES-3DVar. For the data of the GRAPES-3DVar system, the time window is set at 30 minutes plus and minus and the horizontal resolution is 15 km to assimilate the MODIS data for 0540 UTC May 26th. In the scheme of assimilation, the observational error of the MODIS data is 2.5 K. As for the error of the background field, it is statistically formulated using the U.S. National Meteorological Center to define the background error of cloud water, cloud ice and cloud cover to be 20% of their values. The MODIS data has been processed with quality control; when the difference between the simulated background brightness temperature and the observed brightness temperature is more than five times as large as the observation errors, the latter will not be used. A control experiment and assimilating experiment were conducted for the heavy rain process in Guangdong on May 26, 2007; no data were assimilated in the control and the brightness temperature of 0540 UTC from Ch. 27 and Ch. 36 of the MODIS were assimilated once. Fig. 6 gives the cost function of the 3-dimensional variance assimilation system and the variation of its gradients with the iterative steps, which shows that the cost function decreases with the increase of the iterative steps until it satisfies the condition for convergence and completes the whole assimilation process.

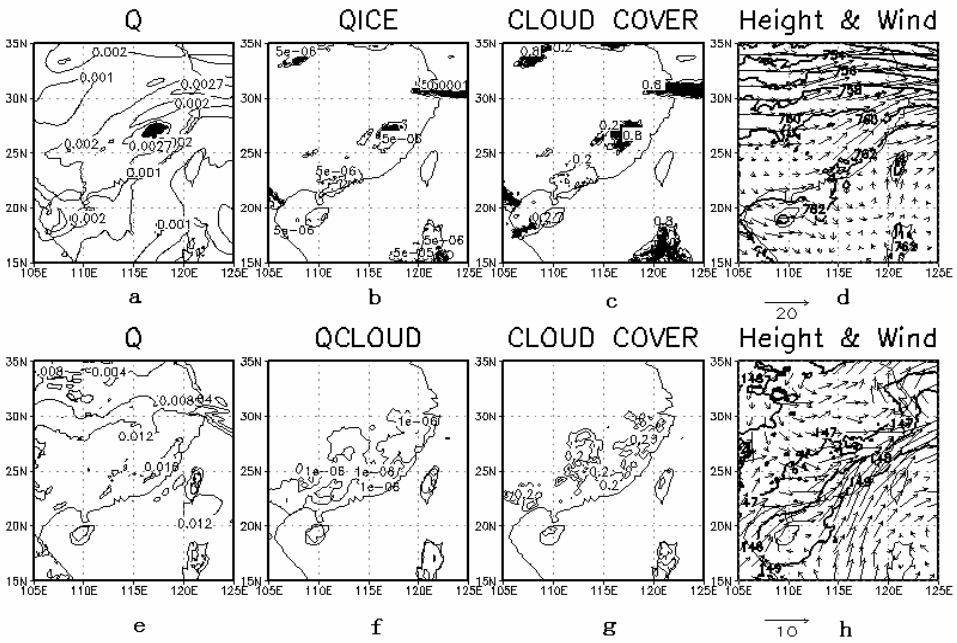


Fig. 5. Specific humidity (a, e), cloud ice-water content (b), cloud water content (f), cloud cover (c, g), geopotential height and wind fields (d, h) at 400 hPa (upper panels) and 850 hPa (lower panels) in the background field for 0600 UTC May 26th. Units: kg/kg (specific humidity); K (temperature); kg/kg (cloud water content); kg/kg (cloud ice-water content); 10 gpm (geopotential height field); m/s (wind field)

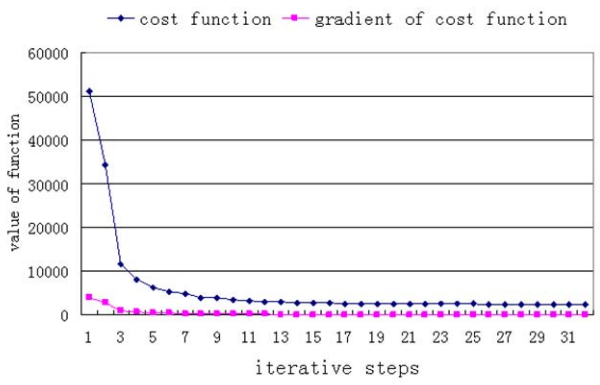


Fig. 6. Values of target functions and their variations in gradient numerals during the minimization.

## 4 ANALYSIS OF RESULTS

Figure 7 presents the increment of the assimilated analysis field relative to the background field, which shows that at 400–300 hPa, specific humidity varies generally in "- + -" alternation, and temperature changes in a pattern of "+ - +", from north to south. In the south of China, specific humidity increases significantly and temperature drops, most notably in northern Guangdong,

accompanying the increase of cloud ice-water content and cloud cover, while upper-level cloud cover and cloud ice-water content decrease in the area of Fujian. As the water vapor, cloud ice-water content and cloud cover are relatively small over Guangdong in the background field but relatively large in the area of Fujian, it is then known that the variations of upper-level specific humidity and cloud cover in the analysis field over these provinces agree with the satellite observations. In the analysis field, specific humidity decreases and temperature rises in the continental region north of 30° N and the ocean south of 20° N. In comparison with the observations from the MODIS instrument (Fig. 4), the regional brightness temperature observed by the satellite is relatively high; the adjustment of temperature and specific humidity will be conducive to the the increase of the regional brightness temperature in the analysis field.

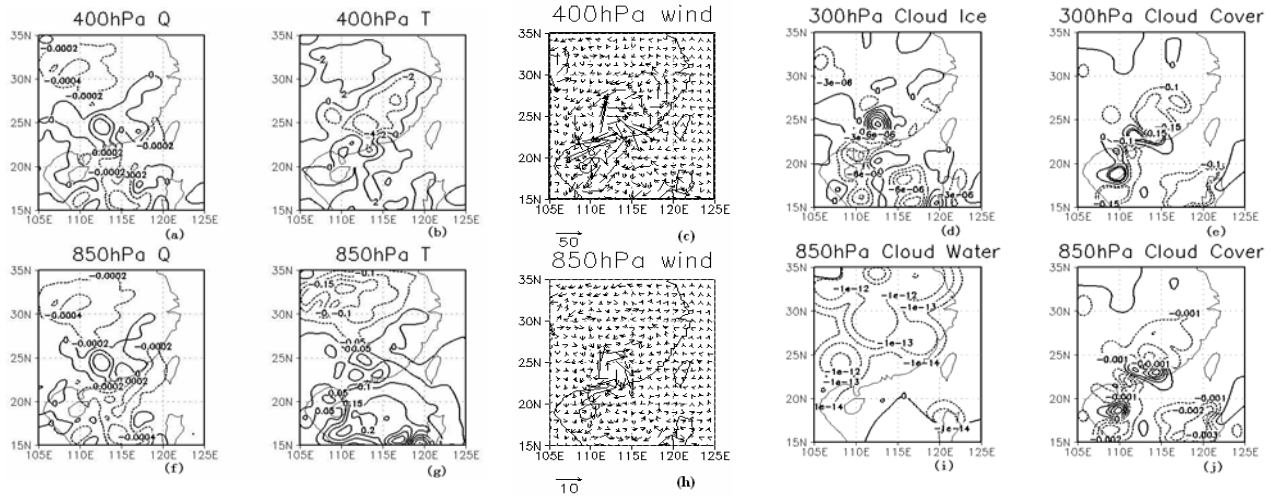


Fig. 7. Increments of specific humidity (a, f), temperature (b, g), wind field (c, h), cloud ice-water content (d), cloud water content (i), cloud cover (e, j) for the analysis field at 400 hPa and 300 hPa (upper panels) and 850 hPa (bottom panels). Units follow those of Fig. 5.

The trend of variation of the lower-level specific humidity is similar to that of the high-level one. Over the Guangdong area, the 850-hPa specific humidity increment is weaker than that at upper levels in terms of area and intensity (Fig. 7f); temperature increment at 850 hPa varies generally from negative in the north to positive in the south, though with small magnitude of value (Fig. 7g); at 850 hPa, cloud water content (Fig. 7i) and cloud cover (Fig. 7j) tend to decrease generally and with small magnitude of value as well.

As the temperature in the analysis field has been adjusted relative to the background field, the wind field is also adjusted accordingly based on the balance equation between the mass and wind fields in the system of GRAPES-3DVar. In the analysis field, well-defined anticyclonic circulation occurs over Guangdong at 400–300 hPa (Fig. 7c), with the location and intensity corresponding to the cloud-derived winds above the level of 400 hPa as observed by the FY-2C satellite (Fig. 1b). By contrast, the background field does not reveal any significant anticyclonic circulation at the upper tropospheric levels over Guangdong. In the analysis field, again, weak increments of cyclonic circulation are observed at the lower tropospheric levels over the province (Fig. 7h) while it is not obviously present in the background field (Fig. 5h). It shows an enhancing trend of lower-level convergence and upper-level divergence in the analysis field relative to the background field over the Guangdong area.

The above variations of the analysis field relative to the background filed suggest that the assimilation of the MODIS data in the cloudy environment is having a great impact on the temperature, specific humidity, wind field, cloud ice-water content and cloud cover at upper levels, and the adjusting trends agree with the observational facts from satellites. Due to the effect of clouds, the low-level adjustment after assimilating the MODIS data is affected just mildly. With the decrease of cloud cover, however, the assimilation begins to have an increasing impact on the low levels. In the clear-sky environment, the assimilation of the MODIS data can adjust the lower-level temperature, specific humidity and wind field.

The adjusted atmospheric and cloud parameters in the analysis field will inevitably affect the simulated brightness temperature. Following the theory of variance assimilation, minimizing the target function during assimilation can reduce the difference between the simulated and observed brightness temperatures. Do Ch. 27 and Ch. 36 assimilated in this study observe this law of change?

The RTTOV radiative transfer model (observational operator) simulates the brightness temperatures using background and analysis fields respectively. By comparing the difference of the simulated brightness temperature prior to and after the assimilation, the results of the assimilation can be verified. Fig. 8 presents comparisons between the simulated and observed brightness temperatures prior to and after the assimilation of Ch. 27 and Ch. 36, where the solid line indicates the tendency. Prior to the assimilation, the brightness temperatures of the two channels as retrieved by the background field are generally low; after the assimilation, the analysis field is closer to the observation. This suggests that the brightness temperatures after the assimilation of these channels have been improved by varying degrees and confirmed that the adjusted temperature, specific humidity and cloud parameters in the analysis field observe the physical law of the radiative transfer model.

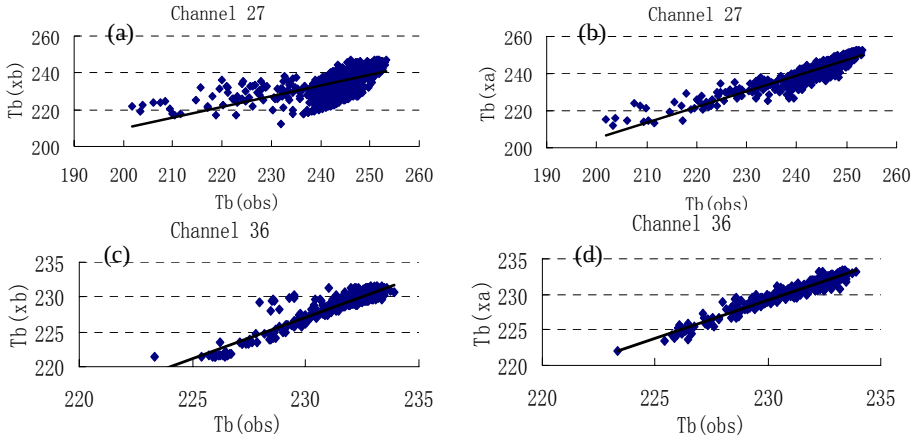


Fig. 8. Comparisons between the brightness temperature of Ch. 27 (a, b) and Ch. 36 (c, d), as simulated by the background field (left panels) and the analysis field (right panels), and those observed. The solid line indicates the trend.

To compare the effect of the MODIS data assimilation scheme, a control experiment and an assimilation experiment are designed. Both of the experiments start integration from 0600 UTC May 26th, with the former assimilating no observations and the latter interpolating the analysis increments to the background. As the rainfall of interest lasted a short duration and confined to a limited area, only the simulated precipitation prior to 1200 UTC May 26th is compared between the two experiments (Fig. 9). The control experiment shows that there is a well-defined rainband from Guangdong to Fujian and the rain begins to weaken after 0900 UTC, matching with the observation as far as the duration is concerned (Fig. 3) but still failing to reflect the center of intense precipitation over the area of Guangdong. The assimilating experiment has roughly the same rainband as the control does and predicts the center of the intense rain over Guangdong with the rain intensity quite consistent with the observation.

With the assimilated MODIS data, the rain intensity is better simulated for Guangdong. Then, how do the adjusted physical quantities of the analysis field affect the model simulation of the rainfall? Part of the clues can be identified in the increment of the analysis field (Fig. 7). The figure shows that in central and northern Guangdong, specific humidity significantly increases from low to high levels of the troposphere and cloud ice-water content increases at upper levels; the sufficient supply of water vapor may be one of the reasons behind the intense rainfall in these parts of the province. Lowered upper-level temperatures and slightly increased lower-level temperatures are just the right allocation to ensure the increase of the atmospheric instability in these regions and might be one of the causes of the appearance of the intense rain. For the wind field, the trends of upper-level divergence and lower-level convergence are conducive to the development of the convective systems over the Guangdong area.

To further study the causes of the analysis field that results in the intense rain, the atmospheric precipitable water and psuedo-equivalent geopotential temperature, $\theta_{se}$, are computed for the time prior to and after the assimilation. Prior to the assimilation, a large region exists from Guangdong to Fujian that has more than 3 centermetres of precipitable water, though without any obvious rain center in Guangdong (Fig. 10a). After the assimilation, however, atmospheric precipitable water increases with the center located in central and northern Guangdong, consistent with the location of an intense rainfall (with a maximum of more than 8 cm) observed by the satellite. See Fig.

10b for the increment of atmospheric precipitable water comparing to that prior to it. It shows that the analysis field has more powerful supply of water vapor in these parts of the province. On the vertical cross section of the increment of $\theta_{se}$ drawn in the direction of the rainband from (20° N, 108° E) to (30° N, 120° E), $\theta_{se}$, in the vicinity of 112° E, decreases at upper levels but increases at mid- and lower-levels, increasing the convective instability. By contrast, $\theta_{se}$, in the area to its northeast, increases at the upper levels but varies insignificantly at the lower levels, which is an allocation that results in the increase of regional stability. The variation of convective stability as shown in that of $\theta_{se}$ is well corresponding to the area of heavy rain in the assimilation experiment, suggesting that the assimilated MODIS data can increase the convective instability in central and northern Guangdong.

With the assimilation of the MODIS data, as shown in the analysis above, the variations of temperature, specific humidity, wind field, cloud water content, cloud ice-water content and cloud cover not only make the analysis-simulated brightness temperature closer to the satellite observation, but also improve the water-vapor supply and increase convective instability in the background field. Compared to the control experiment, the assimilating experiment can yield better forecasts of the location and intensity of the heavy rain in the Guangdong area.

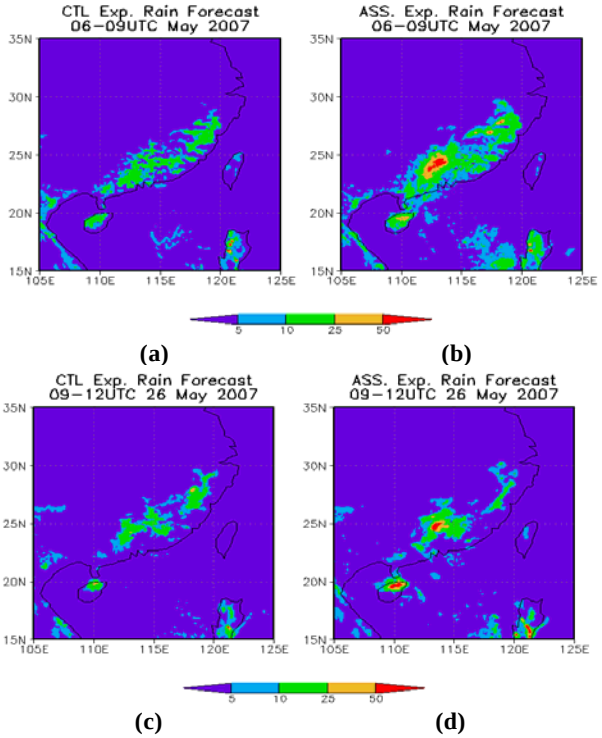


Fig. 9. 3-h cumulative rainfall as simulated by the control experiment and assimilating experiment. Unit: mm. a: control exp., 0600–0900 UTC; b: assimilating exp., 0600–0900 UTC; c: control exp., 0900–1200 UTC; d: assimilating exp., 0900–1200 UTC

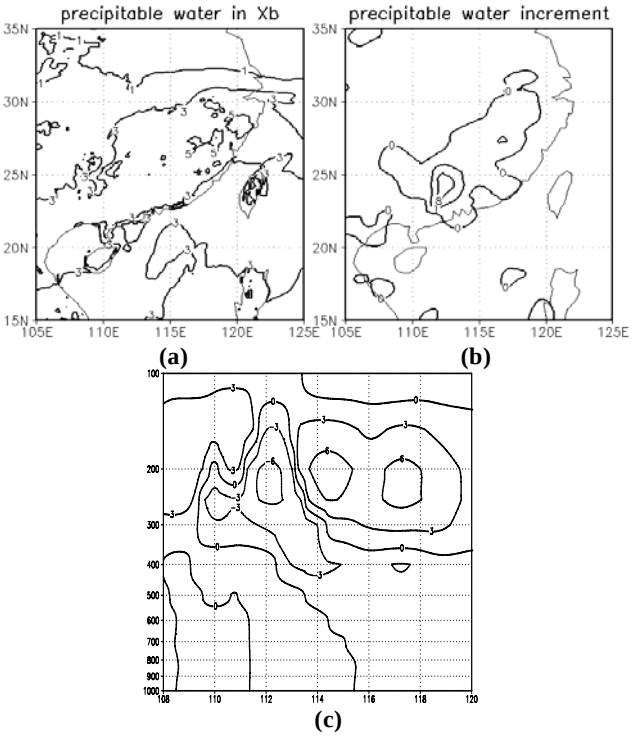


Fig. 10. Distribution of the increments of atmospheric precipitable water (unit: cm) in the background (a) and analysis (b) fields and vertical cross sections (c, unit: K) of the increments of pseudo-equivalent geopotential temperature along (20° N, 108° E) to (30° N, 120° E).

## 5 CONCLUSIONS AND DISCUSSION

Clouds play such an important role in the radiative transfer of the infrared channels that inclusion of cloud parameters in the radiative transfer model of the assimilating system can improve the simulation of the infrared channels of the satellite and increase the accuracy of the observational operator for satellite data assimilation in the assimilation system. With cloud parameters as the governing variables, the assimilation of the MODIS radiative brightness temperature data has improved the results of the analysis and forecast. In this paper, on the basis of GRAPES-3Var runs, cloud water content, cloud ice-water content and cloud cover are added to improve the RTTOV radiative transfer model, and these cloud parameters are then used as the governing variables in the assimilation to define the error arrays for the background field and observations and to determine the quality-control scheme for the observations. Selected for our study is a heavy rain that took place on May 26, 2007 in Guangdong with the background of monsoon circulation in the South China Sea. The 6-h model forecast field was used as the background field. The distribution of water

vapor and upper-level wind fields of the troposphere deviated to some extent from the observation. The brightness temperature of Ch. 27 and Ch. 36 were chosen for assimilation and the WRF model was used in a control and an assimilating experiment.

(1) The assimilated MODIS data can improve the distribution of water vapor and temperature in the initial field and reflect how the water vapor supply and stability distribute in the center of the rain area. The adjustment of the wind field has revealed the characteristics of the troposphere: the upper-level divergence is accompanied by lower-level convergence, and the trend of atmospheric and cloud parameters adjustment is consistent with the observations of the satellite. The brightness temperature as retrieved from the analysis field by the radiative transfer model is superior to that by the background field.

(2) The assimilation experiment can improve short-term forecast of rainfall and have realistic simulation of the position and intensity of the center of the heavy rain over the Guangdong area.

(3) Affected by the upper-level clouds, the assimilated MODIS data adjust the parameters of lower-level clouds less significantly than those of the upper-level clouds; with the decrease of cloud cover, however, the effect on the lower-level clouds is gradually increasing.

While the infrared data have good reproduction of the overall features of the clouds, they cannot describe their inner structure in great detail. As a result, the assimilated MODIS data adjust the lower-level clouds only mildly due to the effect of upper-level clouds. In the future, the results of the assimilation of in-cloud parameters and lower-level clouds need to be improved by combining microwave data with radar data.

## REFERENCES:

[1] LU Da-ren; WANG Pu-cai; QIU Jin-huan, et al. An overview on the research progress of atmospheric remote sensing and satellite meteorology in China [J]. Chin. J. Atmos. Sci., 2003, 27(4): 552-566.

[2] BADER M J, FORBES G S, GRANT J R, et al. Images in weather forecasting - A practical guide for interpreting satellite and radar imagery [M]. LU Nai-meng, et al. (translators) Beijing: Science and Technology Press, 1998.

[3] CHEN Wei-min. Satellite Meteorology (Edition Two) [M]. Beijing: China Meteorological Press, 2005.

[4] SHI Chun-xiang; JIANG Ji-xi, FANG Zong-yi. A Study on the features of severe convective cloud clusters causing serious flooding over Changjiang river basin in 1998 [J]. Clim. Environ. Res., 2000, 5(3): 279-286.

[5] WANG Li-kun, TAO Zu-yu, YANG Yang, et al. Analysis of satellite image characters of severe storm rainfall during the flood of Yangtze river in 1998 [J]. Acta Sci. Nat. Univ. Pek., 2000, 36(1): 87-94.

[6] NI Yun-qi, ZHOU Xiu-ji, ZHANG Ren-he, et al. Experiments and studies for heavy rainfall in southern China [J]. J. Appl. Meteor. Sci., 2006, 17(6): 690-704.

[7] XIONG Wen-bing, LI Jiang-nan, YAO Cai, et al. Analyzing continuous rainstorm in southern China in June 2005 [J]. J. Trop. Meteor., 2007, 23(1): 90-97.

[8] LIAO Guo-nan. Introductions to Atmospheric Radiation (Edition Two) [M]. GUO Cai-li, et al. (translators) Beijing: China Meteorological Press, 2004.

[9] ANDERSSON E, PAILLEUX J, THÉPAUT J-N, et al. Use of cloud-cleared radiances in three/four-dimensional variational data assimilation [J]. Quart. J. Roy. Meteor. Soc., 1994, 120: 627-653.

[10] DERBER J C, WU W. The use of TOVS cloud-cleared radiances in the NCEP SSI analysis system [J]. Mon. Wea. Rev., 1998, 126(8): 2287-2299.

[11] KIDDER S Q, GOLDBERG M D, ZEHR R M, et al. Satellite analysis of tropical cyclones using the advanced microwave sounding Unit (AMSU) [J]. Bull. Amer. Meteor. Soc., 2000, 81(6): 1241-1260.

[12] CHEVALLIER F, KELLY G. Model clouds as seen from space: comparison with, geostationary imagery in the 11-m window channel [J]. Mon. Wea. Rev., 2002, 130(3): 712-722.

[13] DING Wei-yu, WAN Qi-lin. The simulation of typhoon chanchu infrared channels brightness temperature [J]. Chin. J. Atmos. Sci., 2008, 32(3): 572-580.

[14] ERRICO R M. Assimilation of satellite cloud and precipitation observations in numerical weather prediction models: Introduction to the JAS special collection [J]. J. Atmos. Sci., 2007, 64(11): 3737-3741.

[15] GREENWALD T J, HERTENSTEIN R, VUKICEVIC T. An all-weather observational operator for radiance data assimilation with mesoscale forecast models [J]. Mon. Wea. Rev., 2002, 130(7): 1882-1897.

[16] DING Wei-yu, WAN Qi-lin, ZHANG Cheng-zhong, et al. Assimilation of the HIRS/3 data under cloudy conditions and its impacts on Typhoon Chanchu [C]// Proceedings of National Seminar on the Progress of Numerical Prediction and Application. Beijing: China Meteorological Press, 2009: 19-28.

[17] BORMANN N, THÉPAUT J N. Impact of MODIS polar winds in ECMWF's 4DVAR data assimilation system [J]. Mon. Wea. Rev., 2004, 132(4): 929-940

[18] DING Wei-yu, WAN Qi-lin, ZHANG Cheng-zhong et al. MODIS brightness temperature data assimilation under cloudy conditions: Methods and ideal tests [J]. J. Trop. Meteor., 2010, 16(4): 313-324.

[19] LIANG Jian-yin. Report on the Monitoring of Monsoon Onset in May 2007 (Issue 1, 2007) [EB/OL]. Guangzhou: Guangzhou Institute of Tropical and Marine Meteorology, China Meteorological Administration [2007-5-30]. http://218.19.164.219/grapes/jcgb/jcgb0705.htm

**Citation:** DING Wei-yu, WAN Qi-lin, HUANG Yan-yan et al. MODIS brightness temperature data assimilation under cloudy conditions II: Impacts on rainstorm forecasting. *J. Trop. Meteor.*, 2011, 17(3): 221-230.